H each, m, diastereotopic CH_2), 0.95 (t, 3 H, J = 7 Hz, CH_3), 8.78 ppm (d, 1 H, J = 4 Hz, quinoline HC=N-); ^{13}C NMR 28.9 (CH_2, no P or Rh coupling, J_{C-H} = 120 Hz), 11.5 (CH_3, J_{C-H} = 127 Hz), 99.9 ppm (CO, doublet, J = 15 Hz). (No one-bond C-H coupling appeared in the proton-coupled spectrum. Some broading of the resonance occurred, but no two-bond couplings were resolved.) **8**: ^1H NMR 1.10 (t, 3 H, J = 7 Hz, CH_3), 9.22 ppm (d, 1 H, J = 4, quinoline HC=N-). **9**: ^1H NMR 8.94 (d of d, 1 H, J = 4.2, 1.8 Hz HC=N-), 8.2-7.4 (m, 5 H, quinoline ring), 3.45 (q, 2 H, J = 7.3 Hz, CH_2), 1.26 ppm (t, 3 H, J = 7.3 Hz, CH_3); ^{13}C NMR 206.9 (CO), 38.1 (CH_2), 8.5 ppm (CH_3).

Acknowledgment. This work was supported by the National Science Foundation (CHE82-07269) and by the donors of the Petroleum Research Fund, administered by the American Chemical Society. The initial phase of this work was also aided by a Cottrell Research Grant from the Research Corp. The Bruker WM 250 spectrometer was acquired through the generosity of the Montedison Group of Milan and the NSF. Dr. J. Van Epp is thanked for his assistance in the use of the WM 250.

Registry No. 1, 38707-70-9; **1D**, 73038-03-6; 2, 12081-16-2; 3, 90029-03-1; 4, 90029-09-7; 4 (4-Mepy), 95675-39-1; 4 (3,5-Me_2py), 95675-40-4; 4 (4-Me_2Npy), 95693-82-6; **4D**, 95675-41-5; 5, 95693-83-7; 6, 95675-42-6; 6 ($PMePh_2$), 95675-43-7; 6 (P(*p*-$CH_3C_6H_4)_3$), 95675-44-8; 6 (P(*p*-$ClC_6H_4)_3$), 95675-45-9; 7, 95675-46-0; 7 ($PMePh_2$), 95675-47-1; 7 (P(*p*-$MeC_6H_4)_3$), 95675-48-2; 7 (P(*p*-$ClC_6H_4)_3$), 95675-49-3; 8, 95675-50-6; 8 ($PMePh_2$), 95675-51-7; 8 (P(*p*-$MeC_6H_4)_3$), 95675-52-8; 8 (P(*p*-$ClC_6H_4)_3$), 95675-53-9; 9, 90029-06-4; $RhCl(PPh_3)_3$, 14694-95-2; PPh_3, 603-35-0; $PMePh_2$, 1486-28-8; P((*p*-$CH_3C_6H_4)_3$), 1038-95-5; P((*p*-$ClC_6H_4)_3$), 1159-54-2.

Supplementary Material Available: Tables of general temperature factor expressions (Tables A and B), table of root-mean-square amplitudes of thermal vibrations (Table C), table of torsion angles (Table D), and table of observed and calculated structure factors (Table E) (25 pages). Ordering information is given on any current masthead page.

Pyrazolyl-Bridged Iridium Dimers. 7.[1] Synthesis and Properties of Bridge-Substituted Analogues of $[Ir(COD)(\mu\text{-pz})]_2$ (pzH = Pyrazole), the "Mixed-Bridge" Complex $[Ir_2(COD)_2(\mu\text{-pz})(\mu\text{-fpz})]$ (fpzH = 3,5-Bis(trifluoromethyl)pyrazole), and the "Mixed-Metal" Dimer $[IrRh(COD)_2(\mu\text{-pz})_2]$. Crystal and Molecular Structures of Bis(cyclooctadiene)bis(μ-3-phenyl-5-methylpyrazolyl)-diiridium(I) (Dissymmetric Isomer) and Bis(cyclooctadiene)bis(μ-3,4,5-trimethylpyrazolyl)diiridium(I)

Gordon W. Bushnell, D. O. Kimberley Fjeldsted, Stephen R. Stobart,* and Michael J. Zaworotko

Department of Chemistry, University of Victoria, Victoria, British Columbia, Canada V8W 2Y2

Selby A. R. Knox and Kirsty A. Macpherson

Department of Inorganic Chemistry, The University, Bristol BS8 1TS, England

Received August 6, 1984

Fifteen diiridium(I) complexes $[Ir(COD)(\mu\text{-L})]_2$ (**2**-**16**) (COD = cycloocta-1,5-diene) related to the prototypal compound $[Ir(COD)(\mu\text{-pz})]_2$ (**1**, pzH = pyrazole) have been synthesized by Cl displacement by LH from $[Ir(COD)(\mu\text{-Cl})]_2$ (L = 4-methylpyrazolyl (**2**), 3-methylpyrazolyl (**3**), 3,5-dimethylpyrazolyl (**4**), 3,5-diphenylpyrazolyl (**5**), 3-phenyl-5-methylpyrazolyl (**6**), 3-(trifluoromethyl)-5-methylpyrazolyl (**7**), 3,5-bis(trifluoromethyl)pyrazolyl (**8**), 3,4,5-trimethylpyrazolyl (**9**), 3,5-dimethyl-4-bromopyrazolyl (**10**), indazolyl (**11**), 3-(heptafluoropropyl)-5-*tert*-butylpyrazolyl (**12**), 3-(trifluoromethyl)-5-phenylpyrazolyl (**13**), 4-chloropyrazolyl (**14**), 4-iodopyrazolyl (**15**), and 4-nitropyrazolyl (**16**)). The products have been characterized by ^1H and ^{13}C NMR spectroscopy and UV/visible absorption spectrophotometry and have been subjected to study by cyclic voltammetry. Among complexes incorporating unsymmetrically substituted bridging ligands, dimers **3**, **7** and **11** exist as diastereoisomeric mixtures, while for **6** one diastereomer predominates and **12** and **13** appear to be formed as single isomers. The predominant diastereomer of compound **6** has been identified as the dissymmetric isomer (C_2 molecular symmetry); monoclinic, of space group $P2_1/n$ with a = 13.690 (4) Å, b = 14.617 (4) Å, c = 15.749 (10) Å, and β = 96.42 (4)°, in which the Ir_2 separation = 3.079 (2) Å. Intramolecular nonbonding approach to within 2.2 Å of hydrogen atoms attached to opposing terminal COD ligands has been identified in crystals of compound **9**, triclinic, of space group $P\bar{1}$, a = 11.116 (4) Å, b = 13.502 (5) Å, c = 11.006 (4) Å, α = 105.45 (4)°, β = 62.16 (3)°, and γ = 110.07 (4)°, in which the Ir_2 separation is 3.096 (1) Å. A marked increase in $E_{1/2}$ is observed compared with the parent compound **1** accompanying either 3,5 or 4 substitution with electron-withdrawing groups (CF_3 or NO_2) of the bridging pyrazolyl unit. Synthesis of the "mixed-bridge" analogue $[Ir(COD)(\mu\text{-pz})(\mu\text{-fpz})Ir(COD)]$ (**17**) and of the "mixed-metal" complex $[RhIr(COD)_2(\mu\text{-pz})_2]$ (**18**) is described, and stability and NMR properties of both these products are reported.

We are investigating the chemistry of compounds related to the pyrazolyl-bridged diiridium(I) complex $[Ir(COD)(\mu\text{-pz})]_2$ (**1**, COD = cycloocta-1,5-diene, pzH = pyrazole) as a model for electronic communication between

0276-7333/85/2304-1107$01.50/0

Table I. Physical and Analytical Data

compd	color	mp, °C	method[a]	yield %	analysis: calcd C	calcd H	calcd N	found C	found H	found N
$[Ir(COD)(\mu\text{-pz})]_2$ (1)	purple-red	285	A	80	35.96	4.11	7.62	35.72	3.90	7.47
$[Ir(COD)(\mu\text{-4-Mepz})]_2$ (2)[b]	brick red	253	A	78	37.78	4.49	7.34	38.54	4.26	7.34
$[Ir(COD)(\mu\text{-3-Mepz})]_2$ (3)	deep red	233	A	78	37.78	4.49	7.34	37.79	4.45	7.29
$[Ir(COD)(\mu\text{-3,5-Me}_2\text{pz})]_2$ (4)	purple-red	310	A	76	39.48	4.84	7.08	40.79	4.62	7.20
$[Ir(COD)(\mu\text{-3,5-Ph}_2\text{pz})]_2$ (5)	brick red	255	A	74	53.16	4.46	5.39	53.89	4.87	4.08
$[Ir(COD)(\mu\text{-3-Ph-5-Mepz})]_2$ (6)	purple	243	A	75	47.25	4.63	6.12	47.48	4.65	6.15
$[Ir(COD)(\mu\text{-fmpz})]_2$ (7)	red-purple	223	A	68	34.66	3.91	6.21	35.82	3.65	5.86
$[Ir(COD)(\mu\text{-fpz})]_2$ (8)	deep purple	235	A	45	30.89	3.18	5.53	30.56	2.28	5.47
$[Ir(COD)(\mu\text{-3,4,5-Me}_3\text{pz})]_2$ (9)	purple	280	A	72	41.06	5.17	6.84	40.93	5.19	6.84
$[Ir(COD)(\mu\text{-3,5-Me}_2\text{-4-Brpz})]_2$ (10)	brick red	265	A	65	32.84	3.82	5.90	33.21	3.67	5.79
$[Ir(COD)(\mu\text{-ind})]_2$ (11)	purple	293	A	79	43.15	4.10	6.71	43.42	4.22	6.51
$[Ir(COD)(\mu\text{-fbpz})]_2$[c] (12)	mauve		B	14						
$[Ir(COD)(\mu\text{-fppz})]_2$ (13)	purple	254	B	30	42.26	3.55	5.48	41.23	3.26	5.26
$[Ir(COD)(\mu\text{-4-Clpz})]_2$ (14)	brick red	285	A	70	32.87	3.51	6.97	32.85	3.41	6.84
$[Ir(COD)(\mu\text{-4-Ipz})]_2$ (15)	brick red	280	A	60	26.78	2.86	5.68	27.85	2.73	5.55
$[Ir(COD)(\mu\text{-4-NO}_2\text{pz})]_2$ (16)	brick red	315 dec	A	45	32.19	2.95	10.24	31.83	3.24	9.69
$[Ir(COD)(\mu\text{-pz})(\mu\text{-fpz})Ir(COD)]$ (17)	purple	164	*a*	27	33.10	3.24	6.43	33.27	3.09	6.35
$[Ir(COD)(\mu\text{-pz})_2Rh(COD)]$ (18)	crimson	270	*a*	5	40.93	4.68	8.68	40.41	4.69	8.40

[a] See text for details. [b] Abbreviations used to define pyrazolyl ligands are listed in ref 6. [c] Characterized by spectroscopic data.

adjacent metal sites and in relation to reactions requiring participation of both centers in a bimetallic array.[1-5] We have shown previously that substitution of the bridging pz heterocycle (e.g., pyrazolyl A to indazolyl B) can lead to changes in structure[2] or reactivity.[2,3] Here we discuss the properties of a range of bridge-substituted analogues of 1 including several in which an unsymmetrical bridging arrangement results in diastereoisomerism (i.e., configurations C and D); we also describe the isolation of a "mixed-bridge" iridium(I) dimer[3,6] and the "mixed-metal" congener $[RhIr(COD)_2(\mu\text{-pz})_2]$ of compound 1 and its dirhodium isomorph.[2,4]

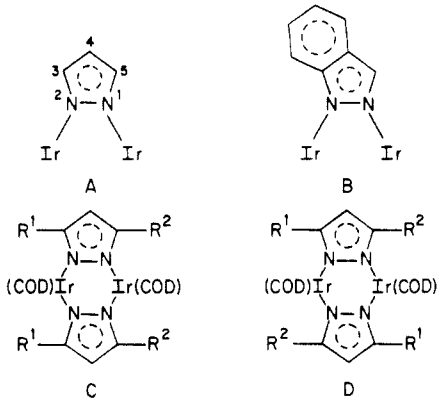

Experimental Section

General procedures have been described in an earlier paper.[1] NMR spectra were recorded by using a Bruker WM250 instrument operating at 250.0 (^{1}H) or 62.9 MHz (^{13}C). UV/visible spectra were measured on a Unicam DU8 spectrophotometer. Electrochemical studies were conducted with a Princeton Applied Research electrochemical system equipped with a Model 175 Universal programmer and a Hewlett-Packard 7040A X-Y recorder. The electrochemical cell consisted of an aqueous standard calomel electrode immersed in a saturated solution in acetonitrile of lithium acetate (reference electrode), a platinum-wire auxilliary electrode, and a platinum foil working electrode. The electrodes were preconditioned in the supporting electrolyte solution, 0.1 M n-Bu_4NClO_4 (TBAP) in degassed acetonitrile, scanning the full potential range several times before addition of the sample under study. Voltammograms of all samples (ca. 10^{-3}M) were recorded at a scan rate of 10 mV s^{-1} under a dry N_2 atmosphere and were introduced as saturated dichloromethane solutions into the supporting electrolyte.

Pyrazole, 3-methylpyrazole, 4-methylpyrazole, and indazole were used as supplied by Aldrich Chemical Co.; 3,5-dimethyl-4-bromopyrazole was purchased from P.C.R. Chemical Inc. With the exception of the 4-chloro, 4-iodo, and 4-nitro compounds, which were prepared by electrophilic substitution of pyrazole,[7,8] the remaining heterocyclic ligands were synthesized by a condensation reaction of the appropriate β-diketone with anhydrous hydrazine.[8] The $[Ir(COD)(\mu\text{-Cl})]_2$ was obtained by the published procedure[9] from $IrCl_3 \cdot 3H_2O$ which was generously loaned by Johnson-matthey Inc.

Synthesis of Compounds. Diiridium(I) Complexes. The synthesis of the parent complex $[Ir(COD)(\mu\text{-pz})]_2$ has been described already.[1] Two slightly different routines were used to obtain the series of analogues listed in Table I, where physical and analytical data are collected and the method of preparation (A or B, see below) for each complex is indicated. Representative reactions are described in full below.

Method A. Bis(cycloocta-1,5-diene)bis[μ-3,5-bis(trifluoromethyl)pyrazolyl]diiridium(I) (8). Excess triethylamine (ca. 1 mL) was added to a solution of $[Ir(COD)(\mu\text{-Cl})]_2$ (100 mg, 0.15 mmol) and 3,5-bis(trifluoromethyl)pyrazole (61 mg, 0.30 mmol) in dry THF (10 mL). After the solution was stirred for 24 h, removal of the solvent was followed by extraction of the residue with hot hexanes (3 × 20 mL) and filtration (4-cm alumina column). Evaporation of solvent and then evacuation (2 h, 10^{-3} mmHg) left a dark residue from which the *product* (68 mg, 0.067 mmol, 45%) was obtained as purple-black crystals by recrys-

(1) Part 6: Atwood, J. L.; Beveridge, K. A.; Bushnell, G. W.; Dixon, K. R.; Eadie, D. T.; Stobart, S. R.; Zaworotko, M. J. *Inorg. Chem.* **1984**, *23*, 4050.
(2) Beveridge, K. A.; Bushnell, G. W.; Stobart, S. R.; Atwood, J. L.; Zaworotko, M. J. *Organometallics* **1983**, *2*, 1447.
(3) Bushnell, G. W.; Fjeldsted, D. O. K.; Stobart, S. R.; Zaworotko, M. J. *J. Chem. Soc., Chem. Commun.* **1983**, 580.
(4) Trofimenko, S. *Inorg. Chem.* **1971**, *10*, 1372.
(5) Marshall, J. L.; Stobart, S. R.; Gray, H. B. *J. Am. Chem. Soc.* **1984**, *106*, 3027.
(6) 3,5-Me_2pzH = 3,5-dimethylpyrazole. Other similar abbreviations used throughout the text are as follows: 4-MepzH = 4-methylpyrazole; 3-MepzH = 3-methylpyrazole; 3,5-Ph_2pzH = 3,5-diphenylpyrazole; 3-Ph-5-MepzH = 3-phenyl-5-methylpyrazole; fmpzH = 3-(trifluoromethyl)-5-methylpyrazole; 3,5-Me_2-4-BrpzH = 3,5-dimethyl-4-bromopyrazole; indH = indazole; fbpzH = 3-(heptafluoropropyl)-5-*tert*-butylpyrazole; fppzH = 3-(trifluoromethyl)-5-phenylpyrazole; 4-ClpzH = 4-chloropyrazole; 4-IpzH = 4-iodopyrazole; 4-NO_2pzH = 4-nitropyrazole.
(7) (a) Huttel, R.; Schafer, O.; Welzel, G. Justus Liebigs *Ann. Chem.* **1956**, *598*, 186. (b) Huttel, R.; Schafer, O.; Jochum, P. *Justus Liebigs Ann. Chem.* **1955**, *593*, 200.
(8) Huttel, R.; Buchele, J. *Chem. Ber.* **1955**, *88*, 1586.
(9) Herde, J. L.; Lambert, J. C.; Senoff, C. V. *Inorg. Synth.* **1974**, *15*, 18.

tallization from a minimum of hot hexane.

Method B. Bis(cycloocta-1,5-diene)bis[μ-3-(heptafluoropropyl)-5-*tert*-butylpyrazolyl]diiridium(I) (12). After 3-(heptafluoropropyl)-5-*tert*-butylpyrazole (90 mg, 0.30 mmol) was stirred with potassium *tert*-butoxide (50 mg, 0.47 mmol) in THF (20 mL) for 10 min, a solution of $[Ir(COD)(\mu\text{-pz})]_2$ (100 mg, 0.149 mmol) was added to the reaction mixture the color of which rapidly darkened to deep purplish red. Further stirring (30 min) was followed by filtration (3-cm alumina column), after which solvent was removed and the residues were extracted with hexanes. The resulting solution was concentrated and loaded onto a 15-cm alumina column, from which elution with hexane yielded the bright purple *product* (25 mg, 0.021 mmol, 14%).

"Mixed-Bridge" Complex [Ir(COD)(μ-pz)(μ-fpz)Ir(COD)] (17). (i) Pyrazole (10 mg, 0.15 mmol), 3,5-bis(trifluoromethyl)-pyrazole (31 mg, 0.15 mmol), and $[Ir(COD)(\mu\text{-Cl})]_2$ (100 mg, 0.15 mmol) were stirred in dry THF (20 mL) with triethylamine (1 mL, excess) for 30 min. The resulting slurry was filtered (3 cm alumina column), and then solvent was removed in vacuo to yield a purple solid. This was washed with cold hexanes (3 × 10 mL), thereby removing the more soluble $[Ir(COD)(\mu\text{-fpz})]_2$ (**8**), and the residue was dissolved in the minimum of THF. Slow addition of hexanes (20 mL) led to formation of dark red crystals of $[Ir(COD)(\mu\text{-pz})]_2$ (**1**) from which the supernatant was carefully removed, filtered, and then pumped to dryness. Dissolution of the solid residue in a minimum of hot hexanes afforded purple crystals of the *product* (35 mg, 0.040 mmol, 27%) on cooling.

(ii) Complex **1** (10 mg, 0.136 mmol) and compound **8** (14 mg, 0.136 mmol) were sealed with THF-d_8 (0.75 mL) in an NMR tube. Monitoring by ^1H NMR spectroscopy showed the mixture to be unchanged after 20 days at ambient. Subsequent heating to 65 °C for 36 h led to a statistical distribution (i.e., 1:2:1) of complexes **1**, **17**, and **8**.

"Mixed-Metal" Complex [Ir(COD)(μ-pz)$_2$Rh(COD)] (18). (i) Excess NEt_3 (ca. 1 mL) was added to a solution of $[Ir(COD)(\mu\text{-Cl})]_2$ (160 mg, 0.24 mmol), $[Rh(COD)(\mu\text{-Cl})]_2$ (118 mg, 0.24 mmol), and pyrazole (70 mg, 1.03 mmol) in dry THF (20 mL). After stirring (30 min), filtration (3-cm alumina column), and removal of solvent, the residue was pumped on (60 min, 10^{-2} mmHg) and then redissolved in the minimum of THF. After slow addition of hexane to form an upper layer, refrigeration at −25 °C led to slow deposition of deep red crystals (262 mg) shown by ^1H NMR spectroscopy to be a statistical mixture of compounds **1**, **18**, and $[Rh(COD)(\mu\text{-pz})]_2$ (**19**).

(ii) Excess of NEt_3 (1 mL) was added to a solution in dry THF (20 mL) of the cationic bis(pyrazole)rhodium complex[10] $[Rh(COD)(pzH)_2]PF_6$ (75 mg, 0.16 mmol) and $[Ir(COD)(\mu\text{-Cl})]_2$. After the mixture was stirred for 30 min, the resulting slurry was filtered through a 3-cm alumina column and the solvent was removed in vacuo. Redissolution of the residues in a minimum of THF followed by addition of hexane then refrigeration afforded orange crystals (50 mg), shown by ^1H NMR spectroscopy to be a mixture of complexes **1**, **18**, and **19** in 20:64:16 proportion.

(iii) The rhodium dimer[11] $[Rh(COD)(\mu\text{-Cl})]_2$ (250 mg, 0.51 mmol) was stirred in a 1:1 mixture of THF/hexanes (10 mL) under an atmosphere of CO gas. When all solid material had dissolved, pyrazole (150 mg, 2.20 mmol) was added and the mixture was stirred for a further 15 min. After concentration to half volume by evacuation removing excess CO, solid $[Ir(COD)(\mu\text{-Cl})]_2$ (350 mg, 0.52 mmol) was added to afford a yellow solution which was stirred for 10 min. On addition of NEt_3 (1 mL, excess) an immediate color change occurred to deep orange-red and NEt_3HCl was precipitated; the slurry was stirred for a further 30 min and then filtered through a short alumina column (3 cm) to give a deep cherry-red solution. Removal of solvent by evacuation then washing with hexanes (3 × 20 mL) was followed by dissolution in the minimum of THF. Hexane was run into the solution carefully to form a second layer after which on refrigeration at −25 °C crimson crystals slowly formed, estimated by ^1H NMR spectroscopy to consist of a 57:43 mixture of the *product* and compound **1**. This mixture (100 mg) was stirred overnight in THF (20 mL) with dmad (dimethyl acetylenedicarboxylate, 5 drops, excess), after which treatment solvent was removed from the orange solution. Recrystallization from a THF/hexane mixture yielded the *product* (30 mg, 0.047 mmol, 5%) as deep red needles together with a pale yellow precipitate (40 mg, 0.46 mmol, 4%) of the dmad adduct[12] of compound **1**.

(iv) A mixture of compound **1** (8 mg, 0.01 mmol) and compound **19** (6 mg, 0.01 mmol) was sealed with THF-d_8 (1 mL) in an NMR tube. After 70 days at ambient, no evidence for the mixed dimer **18** could be detected by ^1H NMR spectroscopy. After 140 days the same technique revealed the presence of ca. 20% complex **18**; subsequent heating to 65 °C (18 h) increased this proportion to ca. 40% and after a further 36 h (65 °C) a statistical mixture of compounds **1**, **18**, and **19** was obtained.

Results and Discussion

The intermediacy of the dimer $[Ir(COD)(\mu\text{-pz})]_2$ (**1**) in the synthesis of the related carbonyl phosphine complex $[Ir(CO)(PPh_3)(\mu\text{-pz})]_2$ (**20**) has been referred to in an earlier paper[1] in this series. Similar bridge substitution of the μ-chloro diiridium precursor $[Ir(COD)(\mu\text{-Cl})]_2$ provides a convenient pathway for synthesis of a family of analogues $[Ir(COD)(\mu\text{-L})]_2$ where L is a C-substituted heterocyclic anion derived from the parent pyrazole $C_3H_4N_2$. Replacement of μ-Cl by μ-L to give in high yield (typically 70%) the appropriate dimeric product occurs readily via abstraction of HCl by triethylamine, except in cases where the bulk of LH intervenes: thus for example with L = 3,5-*t*-Bu$_2$pz, the chloro-bridged starting complex was recovered unchanged. By first forming the pyrazolyl anion by deprotonation of LH using KO-*t*-Bu, it did however prove possible to isolate compounds **12** and **13** in which L = 3-(heptafluoropropyl)-5-*tert*-butylpyrazolyl or 3-(trifluoromethyl)-5-phenylpyrazolyl, although in greatly reduced yield (ca. 30%). In a related context, we have found that treatment[13] of compound **8** (i.e., L = fpz) with CO then PPh_3 affords a mononuclear complex, which has been synthesized independently from *trans*-$[Ir(PPh_3)_2(CO)(Cl)]$ and crystallographically characterized by Bandini et al.[14] Compounds **1**–**11** were identified initially by IR spectra, in which we consider absorption in the 1450–1500 cm^{-1} range to be diagnostic of the bridging ligand, by microanalytical data (Table I), and by NMR measurements which are discussed below. By modifying the synthetic procedure through introduction in equimolar ratio of two different pyrazoles, L = pz and fpz, a mixture of all three possible binuclear products was obtained, from which the "mixed-bridge" complex **17** could rather easily be separated by crystallization, taking advantage of the marked difference in solubility in hexane between the bis(μ-fpz) analogue **8** and the parent dimer **1**.

The dirhodium analogue **19** of compound **1**, which has recently been crystallographically characteized in our laboratory,[2] was first prepared in 1972 by Trofimenko.[4] The markedly lower reactivity of this complex compared[2] with related diiridium(I) compounds including **1** and **20** both of which[1,12] readily undergo two-center oxidative-addition reactions, led us to seek a route to the corresponding mixed-metal congener $[RhIr(COD)_2(\mu\text{-pz})_2]$ (**18**). Such heterobimetallic d^8 species have proven difficult to isolate[15,16] in the absence of specific reactions designed to

(10) Decker, M. J.; Fjeldsted, D. O. K.; Stobart, S. R., unpublished results. Data for $[Rh(COD)(pzH)_2]PF_6$. Anal. Calcd for $C_{14}H_{20}F_6N_4PRh$: C, 34.14; H, 4.10; N, 11.38. Found: C, 34.02; H, 3.98; N, 11.31. See also: Decker, M. J.; Fjeldsted, D. O. K.; Stobart, S. R.; Zaworotko, M. J. *J. Chem. Soc., Chem. Commun.* **1983**, 1525.

(11) Chatt, J.; Venanzi, L. M. *J. Chem. Soc.* 1957, 4735.

(12) Coleman, A. W.; Eadie, D. T.; Stobart, S. R.; Zaworotko, M. J.; Atwood, J. L. *J. Am. Chem. Soc.* **1982**, *104*, 922.

(13) Coleman, A. W.; Fjeldsted, D. O. K.; Stobart, S. R., unpublished observations.

(14) Bandini, A. L.; Banditelli, G.; Bonati, F.; Demartin, F.; Manessero, M.; Minghetti, G. *J. Organomet. Chem.* **1982**, *C9*, 238.

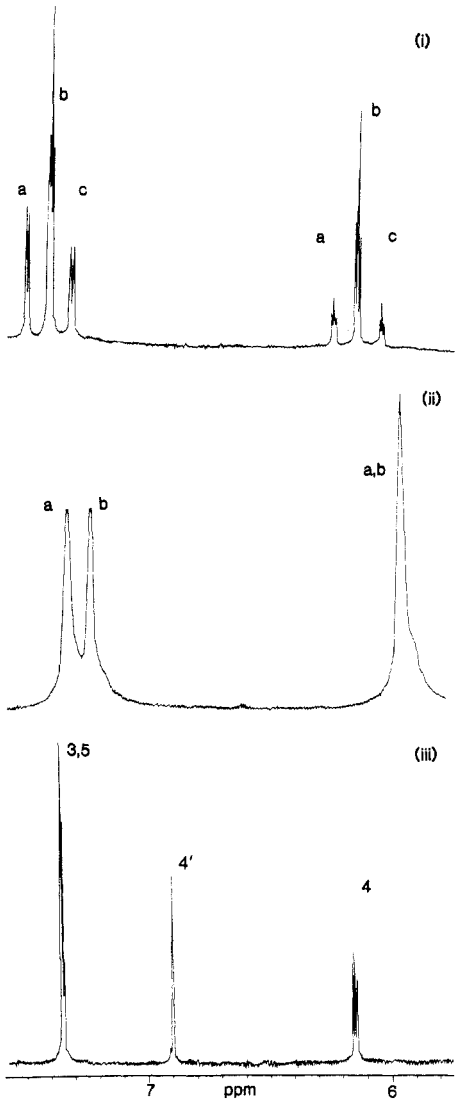

Figure 1. Hydrogen-1 NMR spectra (250 MHz) in the δ 5.8–7.5 range for (i) a mixture of $[Ir(COD)(\mu\text{-pz})]_2$ (a), $[RhIr(COD)_2(\mu\text{-pz})_2]$ (b), and $[Rh(COD)(\mu\text{-pz})]_2$ (c), (ii) $[Ir(COD)(\mu\text{-3-Mepz})]_2$ (mixture of diastereomers a and b), and (iii) $[Ir(COD)(\mu\text{-pz})(\mu\text{-fpz})Ir(COD)]$: $H^{3,5}$ and H^4 of μ-pz and $H^{4'}$ of μ-fpz.

link the two metal-containing fragments, although very recently Shaw and co-workers[17] have described methods for assembling such bis(phosphine)-bridged binuclear compounds: accordingly addition of pyrazole and then excess NEt_3 to solutions containing equimolar amounts of the two precursors $[M(COD)(\mu\text{-Cl})]_2$ (M = Rh, Ir) afforded only a statistical distribution of all three possible products. This was established by using ^1H NMR spectroscopy as discussed below (see Figure 1i). Since attempts at chromatographic separation of the mixture of the Rh–Ir complex **18** with compounds **1** and **19** proved to be unsuccessful, the reactivity of the cationic rhodium(I) pyrazole complex[10] $[Rh(COD)(pzH)_2]PF_6$ toward $[Ir(COD)(\mu\text{-Cl})]_2$ was investigated; treatment of a solution of these two components with NEt_3 still afforded a mixture, however, although the proportion of the desired product **18** was observed to increase at the expense of that of **19**. We attribute the poor selectivity in this experiment to the lability of N-bonded pzH in mononuclear Rh(I) complexes, a phenomenon we are currently examining in a continuing study.[10]

The low solubility of compounds **1** and **19** in hexane contrasts with that[18] of $[Rh(CO)_2(\mu\text{-pz})]_2$ and suggested an alternate approach to a "mixed-metal" species. Carbonylation in situ of $[Rh(COD)(\mu\text{-Cl})]_2$ in THF/hexane followed by addition of pyrazole then $[Ir(COD)(\mu\text{-Cl})]_2$ and NEt_3 appeared to be accompanied by extensive decomposition but after workup yielded a THF-soluble fraction free of dirhodium products. A chemical strategy was used to deal with the remaining mixture, which consisted of compounds **1** and **18**: the former readily forms a separable 1:1 adduct[12] with dimethyl acetylenedicarboxylate, a reagent which proved to be without effect on the heterobimetallic congener. In this manner the latter was isolated pure, although in practical terms in unacceptably low overall yield. The formation of the rhodium COD compound from a carbonyl precursor is fortuitous but not without precedent.[19] By monitoring the behavior (^1H NMR) of an equimolar mixture of the homobimetallic complexes **1** and **19** it was established that dismutation to form compound **18** was very slow under ambient conditions. A similar NMR experiment showed that equilibration of complexes **1** and **8** to give the "mixed-bridge" compound[3] **17** was likewise very slow.

NMR data for compounds **1**–**18** prove to be extremely useful as a means for establishing stereochemistry: in particular, in ^1H spectra the signals arising from protons attached to the C^{3-5} part of the bridging framework are well-separated from other features (see Figure 1) while in ^{13}C spectra resonances due to the terminal COD ligands are easily distinguishable from one another. In this way modification to the structure[2] of complex **1** which reduces the molecular symmetry either along or perpendicular to the intermetallic axis may readily be distinguished. Multiplets attributable to the bridge $H^{3,5}$ pair (doublet) coupled to H^4 (triplet) for the M_2 analogues **1** and **19** (i.e., M = Ir and Rh, respectively) are chemically shifted from one another by ca. 0.2 ppm but interestingly in the "mixed-metal" congener **18** the nondegeneracy introduced between hydrogens at bridge 3,5-positions is marginal even at 250 MHz, generating an apparent triplet composed of overlapping doublets; the chemical shift data do however show a monotonic variation along the series, as is illustrated in Figure 1i for a mixture of the three complexes which is considerably enriched in compound **18** compared with the statistical distribution.

Diastereoisomerism resulting from unsymmetrical bridge substitution is evident in the ^1H NMR spectrum of compound **3**, derived from 3-MepzH: doublets at δ 7.32 and 7.22 may be assigned to H^5 resonances in the two different isomers (distribution of which appears to be equal on the basis of peaks heights, Figure 1ii) with differentiable 3-Me signals at δ 2.36 and 2.34. No corresponding separation could be resolved, however, between bridge H^4 environments, either for complex **3** (Figure 1ii) or any of the unsymmetrically 3,5-disubstituted analogues. Isomer ratios for the latter were determined from proton signals due to bridge substituents or by recourse to ^{13}C NMR spectra. Thus a 1:1 diastereomer distribution is indicated for complex **7**, L = fmpz (δ_{Me} 2.42, 2.40), while a 1:3 mixture was identified for compound **11**, L = ind, on the basis of two

(15) Evans, G. O.; Sheline, R. K. *J. Inorg. Nucl. Chem.* **1968**, *30*, 2862.
(16) Abel, E. W.; Stone, F. G. A. *Q. Rev., Chem. Soc.* **1970**, *24*, 498. Gladfelter, W. L.; Geoffroy, G. L. *Adv. Organomet. Chem.* **1980**, *18*, 207.
(17) Pringle, P. G.; Shaw, B. L. *J. Chem. Soc., Chem. Commun.* **1982**, 81.

(18) The complex $[Rh(CO)_2(\mu\text{-3,5-Me}_2\text{pz})]_2$ was first reported by Trofimenko (see ref 4), and the μ-pz analogue may be obtained by using the same synthetic route. The X-ray crystal structure of $[Rh(CO)_2(\mu\text{-pz})]_2$ has recently been determined: Storr, A., private communication.
(19) Bonnet, J. J.; Galy, J.; deMontauzon, D.; Poilblanc, R. *J. Chem. Soc., Chem. Commun.* **1977**, 47. Uson, R.; Oro, L. A.; Ciriano, M. A.; Bello, M. C. *J. Organomet. Chem.* **1982**, *240*, 199.

Table II. ^1H and ^{13}C NMR Data[a] for Diiridium(I) Complexes 1, 2, 4, 5, 8-10, and 14-16

	^1H/ppm				^{13}C/ppm			
compd	$\delta(H^{3,5})$	$\delta(H^4)$	δ(COD)[b]	δ(R)	$\delta(C^{3,5})$	$\delta(C^4)$	δ(COD)	δ(R)
1[c]	7.48 d	6.22 t	4.01, 3.48, 2.49, 1.80		136.4	106.4	68.3, 65.1, 33.0, 32.3	
2[d]	7.27		3.97, 3.45, 2.48, 1.86	1.98	135.7	115.8	67.0, 64.1, 32.4, 31.6	9.1
4[d]		5.72	4.23, 3.78, 2.58, 1.89	2.34	145.7	104.6	66.3, 63.6, 32.4, 31.9	13.9
5		6.42	4.72, 3.70, 2.30, 1.60	8.05,[b] 7.40[b]	152.1	107.6	67.1, 64.0, 32.1, 30.6	134.2, 128.5, 127.9, 127.8
8		6.82	4.59, 4.06, 2.62, 2.48		141.7	108.0	69.7, 65.2, 32.0, 31.1	120.3
9[d]			4.19, 3.70, 2.55, 2.36	2.26 1.77	143.4	110.6	66.0, 63.4, 32.4, 31.8	12.7, 8.6
10			4.23, 3.82, 2.57, 2.39	2.32	144.1	93.6	67.0, 64.2, 32.3, 31.7	13.4
14[e]	7.43		3.96, 3.55, 2.47, 1.86					
15[e]	7.48		3.99, 3.55, 2.45, 1.60					
16	8.14		4.02, 3.72, 2.47, 1.92		135.4	*f*	70.7, 66.8, 32.3, 31.5	

[a] δ measured high frequency (equivalent to downfield) positive vs. Me_4Si in $CDCl_3$ solution unless otherwise indicated. Signals are singlets unless otherwise indicated. Labeling $H(C)^{3,5}$, $H(C)^4$ pyrazolyl bridging ligand; COD = cycloocta-1,5-diene ligand; R = bridge Me, CF_3, or Ph substituent. [b] Complex multiplet envelopes. [c] ^1H and ^{13}C in CD_2Cl_2 solution. [d] ^1H in CD_2Cl_2 solution. [e] Insufficient solubility for ^{13}C NMR measurements. [f] Resonance not observed.

appropriate superimposed ^{13}C patterns. One isomer of complex **6**, which from ^{13}C NMR data predominates almost to the exclusion of the other, has been structurally characterized by X-ray methods (see below); compounds **12** and **13** seem again from NMR measurements to adopt a single configuration, either C or D. Full data for all of the new compounds are presented in Tables II and III, providing for convenience a division between complexes possessing symmetrically or unsymmetrically substituted bridging ligands. The ^1H NMR spectrum of the "mixed-bridge" compound **17** shows[3] three signals in the pyrazolyl region: a doublet ($H^{3,5}$) and triplet (H^4) array corresponding to the unsubstituted bridging ligand, together with a singlet due to H^4 of the fpz unit. A downfield shift of ca. 1 ppm in the H^4 resonance which accompanies CF_3 substitution (Figure 1iii) is parallelled in other analogues incorporating electron-withdrawing bridge substituent groups (Tables II and III).

The low-energy region of the electronic absorption spectrum of compound **1** has been assigned[5] by analogy with analysis of related data for "face-to-face" d^8–d^8 bimetallic systems which have higher symmetry[20] and exhibit demonstrable[21] interaction between the adjacent metal centers. Two characteristic bands are observed for each of the dimers **1**–**18**, near 380 and 500 nm. There is little evidence for a systematic energy dependence upon the bridge substitution pattern (Table IV) although there is considerable variation in ϵ_{max} for both features. The absorption at longer wavelength (in the range 498–530 nm) is attributable[5] to the singlet $^1B_2$ component of a $d\sigma^*$–$p\sigma$ transition under C_{2v} symmetry. Emission from this state was detected (THF solution, Aminco SPF-125 spectrofluorometer) in the range 540–598 nm and also from the corresponding triplet $^3B_2$ state (excitation into which gives rise to low-intensity absorption[5]) ca. 100 nm to lower energy (650–705 nm). An obvious blue shift in the energy of $^1B_2$ of $d\sigma^*$–$p\sigma$ (Table IV) is also striking within the series **1**, **18**, and **19** (i.e., Ir_2, RhIr, and Rh_2).

A study of the temperature dependence of the triplet lifetime has been used to relate in energetic terms the ground-state Ir_2, the excited-state Ir_2*, and the oxidized form Ir_2^+ for $[Ir(COD)(\mu\text{-pz})]_2$ in terms of a modified Latimer diagram.[5] To assess the influence of bridge substitution on the oxidation process each of the complexes **1**–**19** was subjected to cyclic voltammetry. Reversible oxidation waves were observed below 0.6 V (Table IV), corresponding to the process Ir_2/Ir_2^+; no second oxidation step could be detected out to ca. 2 V, although for complexes with phenyl bridge substituents secondary irreversible processes were apparent with $E_{1/2}$ near 1 V vs. SSCE. The data of Table IV show that substitution in the bridge 3,5-positions with either Ph or CF_3 has a considerable effect on $E_{1/2}(Ir_2/Ir_2^+)$, with an increase from 0.22 V for the parent complex **1** to 0.39 V for **5** and 0.59 V for **8**, while incorporation of Me produces little variation. The observed trend, i.e., smaller change with Ph than CF_3 but in the same sense, is consistent[22] with σ inductive electron withdrawal from the pyrazolyl ring system. Substitution of H or Me at the 4-position by Cl or I induces little change in $E_{1/2}$, but the latter is strongly influenced by introduction of the more electron-withdrawing nitro group (Table IV). Significantly, therefore, these data offer clear evidence for electronic communication between the Ir centers via orbital interaction with the bridging ligand.

X-ray Crystal Structure Determinations for Compounds 6 and 9

Data Collection and Refinement. A single crystal of compound **6**, purple-black lozenges, was sealed in a thin-walled glass capillary; after determination of unit cell parameters by Weissenberg and precession camera techniques, the crystal was placed on a Picker four-circle diffractometer automated with a PDP-11/10 computer (University of Victoria). Lattice parameters determined accurately from 16 reflections with $2\theta > 25°$ are given in Table V together with other related data. Following correction of intensities for Lorentz, polarization, and absorption effects the structure was solved by using the direct methods program package MULTAN.[23] Least-squares refinement of the resulting model was accomplished by using SHELX.[24] Following anisotropic refinement of all non-hydrogen atoms, the COD methyne hydrogens were located on a difference Fourier map and fixed to the appropriate carbon atoms. With other hydrogen atoms placed in calculated positions refinement converged to give final values of $R = \sum ||F_o| - |F_c||/\sum|F_o| = 0.032$ and $R_w = [\sum w(F_o - F_c)^2/\sum w(F_o)^2]^{1/2} = 0.034$.

A black crystal of complex **9** (from CH_2Cl_2/ether) was similarly mounted and placed directly upon a Nicolet P3m diffractometer

(20) Rice, S. F.; Gray, H. B. *J. Am. Chem. Soc.* **1981**, *103*, 1593.
(21) Dallinger, R. F.; Miskowski, V. M.; Gray, H. B.; Woodruff, W. H. *J. Am. Chem. Soc.* **1981**, *103*, 1595.
(22) Lowry, T. H.; Richardson, K. S. "Mechanism and Theory in Organic Chemistry", 2nd ed.; Harper and Row: New York, 1981; p 139.
(23) Germain, G.; Main, P.; Woolfson, M. M. *Acta Crystallogr., Sect. A* **1971**, *A27*, 368.
(24) SHELX, a system of computer programs for X-ray structure determination by G. M. Sheldrick, 1976. Other programs used on an IBM 4341 computer include ORTEP (thermal ellipsoid plots, by C.K. Johnson) and local versions by G. W. Bushnell for hydrogen atom position calculations, best least-squares planes calculations, and table generation.

Table III. ^1H and ^{13}C NMR Data[a] for Compounds 3, 6, 7, 11–13, 17, and 18

	^1H/ppm				^{13}C/ppm			
compd	$\delta(H^{3,5})$	$\delta(H^4)$	$\delta(COD^b)$	$\delta(R)$	$\delta(C^{3,5})$	$\delta(C^4)$	$\delta(COD)$	$\delta(R)$
3[c]	7.32 d, 7.22 d	5.95 d	4.10, 3.73, 2.49, 1.83	2.36, 2.34	145.6, 145.0, 136.0	104.8	67.7, 64.9, 32.6, 32.2, 31.7	14.5, 13.9
6		6.15	4.38, 3.84, 3.72, 3.57, 3.38, 2.53, 1.82	8.13,[b] 7.35,[b] 2.63	149.9, 146.3	106.1	68.2, 66.3, 64.4, 63.5, 32.1, 30.6	134.6, 127.8, 127.2, 14.6
7		6.23	4.60, 4.20, 3.90, 2.60, 2.40, 1.80	2.42, 2.40	147.0	105.9	69.1, 67.0, 65.4, 63.2, 32.6, 32.0, 31.8, 31.1	*d* 14.0
11[e]	7.99		4.60, 4.40, 3.95, 3.60, 2.75, 2.05	7.75, 7.54, 7.17, 6.88				
12		6.35	5.03, 4.21, 3.75, 3.52, 2.64, 2.49, 1.89	1.33	163.2	107.1	69.3, 64.8, 63.8, 62.4, 32.6, 32.0, 31.8, 29.6	*f* 32.0, 14.1
13		6.15	4.75, 3.92, 3.72, 3.36, 2.52, 2.32, 1.92, 1.71	8.18,[b] 7.45[b]	151.7	107.5	77.5, 77.0, 64.9, 64.2, 32.2, 31.6, 31.2, 30.5	132.9, 128.2, 127.9, 140.7
17[g]	7.34 d	6.89, 6.15 t	4.35, 4.28, 4.08, 3.45, 2.55, 2.42, 1.94, 1.87		140.8, 135.2	107.8, 105.6	69.4, 67.5, 66.6, 62.2, 32.4, 32.2, 31.6, 31.3	120.7
18	7.40 t	6.15 t	4.28, 4.03, 3.80, 3.63, 2.65, 2.46, 1.96, 1.82		137.1, 136.4	104.8	82.1, 82.0, 80.7, 80.6, 66.9, 64.5, 32.6, 31.4	

[a] See footnote *a*, Table II. [b] Complex multiplet contour. [c] ^1H NMR in CD_2Cl_2 solution. [d] CF_3 resonance not observed. [e] ^{13}C NMR not assigned in detail but showed evidence for two diastereomers, see text. [f] $CF_2CF_2CF_3$ resonances not observed. [g] ^1H and ^{13}C NMR in CD_2Cl_2 solution.

Table IV. Visible Absorption Spectra[a] and Redox Potential Data

compd	λ_{max}/nm ($\epsilon \times 10^{-3}$)	$E_{1/2}$/V[b]
1	381 (2.55), 500 (7.77)	0.22
2	385 (2.01), 501 (5.53)	0.22
3	430 (4.61), 510 (4.83)	0.27
4	391 (1.39), 528 (8.57)	0.25[c]
5	380 (2.94), 499 (9.68)	0.39[c]
6	388 (4.45), 531 (17.10)	0.31
7	388 (1.56), 524 (9.09)	0.46
8	390 (0.85), 521 (4.23)	0.59
9	391 (1.19), 530 (6.26)	0.26
10	391 (1.73), 529 (9.68)	0.35[c]
11	388 (6.12), 520 (14.60)	0.20[c]
12	381 (2.83), 531 (13.50)	0.33
13	385 (2.40), 526 (8.82)	0.44
14	381 (1.77), 498 (3.24)	0.23
15	385 (2.16), 502 (6.38)	0.22[c]
16	425 (3.17), 505 (1.97)	0.37
17	379 (2.41), 501 (6.95)	*d*
18	373 (1.72), 471 (4.07)	0.45[c]
19	381 (3.60), 443 (8.11)	0.45[c]

[a] Measured in THF solution. [b] Vs. SSCE, measured as described in Experimental Section. Observed cyclic voltammetric behavior reversible unless otherwise indicated. [c] Irreversible oxidation wave. [d] Not measured.

Table V. Crystal Data and Summary of Intensity Data Collection and Structure Refinement for Compounds 6 and 9

	6	9
formula	$C_{36}H_{42}N_4Ir_2$	$C_{28}N_{42}N_4Ir_2$
mol wt	915.2	819.1
diffractometer	Nicolet P3m	Picker
cryst system	monoclinic	triclinic
space group	$P2_1/n$	$P\bar{1}$
cell dimens,		
a, Å	13.690 (4)	11.116 (4)
b, Å	14.617 (4)	13.502 (5)
c, Å	15.749 (10)	11.006 (4)
α, deg	90	105.45 (4)
β, deg	96.42 (4)	62.16 (3)
γ, deg	90	110.07 (4)
cell vol, Å^3	3132	1367
Z	4	2
ρ(calcd), g cm^{-3}	1.94	1.99
μ(calcd), cm^{-1}	84.9	103.3
radiatn	Mo Kα	Mo Kα
stds	2 every 50	3 every 50
std decay	±1.5%	±2%
2θ range deg	4–50	4–50
obsd reflctns	4390	3709
no. of parameters varied	379	307
R	0.042	0.032
R_w	0.043	0.034

(University of Bristol). Crystal data and collection parameters are summarized in Table V. Similar treatment of data to that described above led to solution of the structure using the heavy-atom method and refinement by least squares.[25] Anisotropic refinement of all non-hydrogen atoms with hydrogens placed in calculated positions gave final values for *R* and R_w of 0.042 and 0.043, respectively.

Neutral atom scattering factors for Ir, N, and C were taken from the compilations of Cromer and Mann[26] with those for H from ref 27. Non-hydrogen atoms were corrected for the real

(25) Computations were carried out within the laboratory using an Eclipse (Data General) mionicomputer with the SHELXTL system of programs (G. M. Sheldrick, SHELXTL, a system of crystallographic programs for use with the Nicolet X-ray system, Cambridge, 1979; updated Gottingen, 1980).

(26) Cromer, D. T.; Mann, B. *Acta Crystallogr., Sect. A* **1968**, *A24* 321.

(27) "International Tables for X-ray Crystallography"; Kynoch Press: Birmingham, England, 1962; Vol. III.

Table VI. Atomic Coordinates (×10⁴) and Isotropic Thermal Parameters (Å² × 10³) for Compound 6

	x	y	z	U,[a] Å²
Ir(1)	4128 (1)	1233 (1)	2975 (1)	36 (1)
Ir(2)	2158 (1)	1159 (1)	3745 (1)	35 (1)
N(1)	2895 (6)	1086 (5)	2064 (5)	42 (3)
N(2)	2041 (5)	994 (5)	2426 (4)	35 (2)
C(1)	3478 (9)	1011 (8)	607 (6)	62 (4)
C(2)	2685 (9)	975 (6)	1187 (7)	56 (4)
C(3)	1713 (8)	768 (7)	1026 (6)	49 (4)
C(4)	1316 (7)	775 (6)	1782 (6)	44 (3)
C(5)	279 (7)	550 (6)	1905 (7)	45 (3)
C(6)	−454 (8)	645 (7)	1245 (7)	55 (4)
C(7)	−1398 (8)	392 (7)	1330 (8)	63 (4)
C(8)	−1652 (8)	81 (8)	2108 (8)	69 (5)
C(9)	−935 (8)	−32 (9)	2766 (8)	68 (5)
C(10)	45 (8)	184 (8)	2675 (7)	59 (4)
N(3)	3738 (5)	−61 (4)	3371 (5)	38 (3)
N(4)	2926 (5)	−92 (5)	3789 (5)	40 (3)
C(11)	1909 (9)	−1267 (7)	4443 (8)	63 (4)
C(12)	2766 (7)	−960 (6)	4011 (6)	42 (3)
C(13)	3483 (7)	−1508 (6)	3721 (6)	46 (3)
C(14)	4076 (7)	−915 (6)	3321 (5)	37 (3)
C(15)	4914 (7)	−1159 (6)	2835 (6)	41 (3)
C(16)	5536 (7)	−1875 (7)	3091 (7)	50 (4)
C(17)	6305 (8)	−2119 (8)	2608 (8)	65 (5)
C(18)	6432 (8)	−1661 (8)	1891 (7)	63 (4)
C(19)	5829 (9)	−951 (8)	1624 (8)	66 (5)
C(20)	5063 (8)	−691 (7)	2092 (7)	54 (4)
C(21)	5620 (7)	1063 (7)	3555 (7)	52 (4)
C(22)	5037 (8)	1467 (7)	4151 (6)	50 (3)
C(23)	5071 (10)	2450 (7)	4412 (8)	70 (5)
C(24)	4884 (10)	3103 (8)	3672 (8)	72 (5)
C(25)	4319 (8)	2682 (6)	2899 (7)	51 (4)
C(26)	4786 (8)	2244 (7)	2257 (7)	56 (4)
C(27)	5879 (9)	2092 (10)	2308 (10)	89 (6)
C(28)	6311 (10)	1591 (10)	3112 (9)	85 (6)
C(31)	1820 (7)	1006 (7)	5018 (5)	47 (3)
C(32)	2602 (8)	1595 (7)	5021 (5)	49 (3)
C(33)	2532 (10)	2626 (8)	5143 (7)	67 (5)
C(34)	2283 (10)	3148 (8)	4322 (8)	74 (5)
C(35)	1806 (8)	2573 (6)	3623 (7)	51 (4)
C(36)	929 (8)	2072 (7)	3652 (7)	54 (4)
C(37)	405 (9)	2035 (9)	4438 (8)	72 (5)
C(38)	786 (8)	1322 (8)	5087 (8)	67 (5)

[a] Equivalent isotropic U defined as one third of the trace of the orthogonalized U_{ij} tensor.

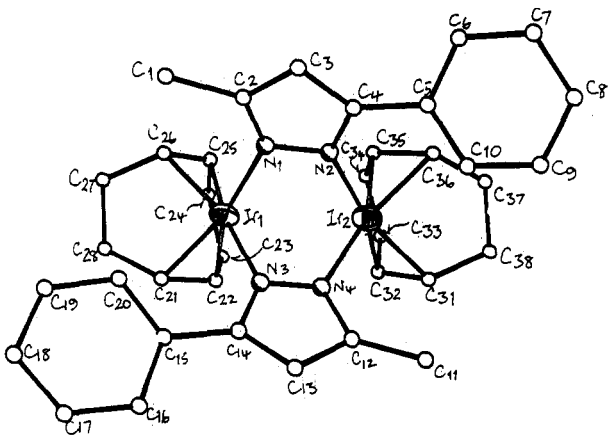

Figure 2. Molecular geometry of compound 6.

and imaginary components of anomalous dispersion.[28] Fractional coordinates for compounds 6 and 9 are listed in Tables VI and VII, respectively. Important bond distances and angles are set out in Table VIII; full data are available in the supplementary material.

(28) Cromer, D. T.; Liberman, D. *J. Chem. Phys.* **1970**, *53*, 1891.

Table VII. Fractional Atomic Coordinates and Temperature Parameters for Compound 9

atom	x/a	y/b	z/c	U_{eq}, Å²
Ir(1)	56968 (3)	26967 (3)	5679 (3)	388 (2)
Ir(2)	25445 (3)	26211 (3)	18444 (3)	380 (2)
N(1)	4474 (7)	1885 (5)	2295 (7)	40 (3)
N(2)	3079 (6)	1903 (5)	2901 (7)	41 (3)
C(1)	2416 (8)	1475 (7)	4101 (8)	40 (4)
C(2)	3376 (10)	1134 (7)	4272 (8)	45 (4)
C(3)	4675 (8)	1426 (7)	3110 (9)	44 (4)
C(4)	950 (10)	1522 (10)	5110 (10)	70 (5)
C(5)	3141 (12)	627 (9)	5474 (10)	68 (6)
C(6)	6077 (10)	1364 (9)	2855 (11)	60 (5)
N(3)	5173 (7)	4027 (5)	1897 (7)	44 (3)
N(4)	3761 (7)	4003 (6)	2468 (7)	44 (4)
C(7)	3518 (10)	4842 (7)	3468 (9)	51 (4)
C(8)	4806 (11)	5419 (7)	3533 (10)	57 (5)
C(9)	5784 (10)	4881 (8)	2573 (10)	51 (5)
C(10)	2066 (12)	4961 (9)	4366 (11)	73 (6)
C(11)	5039 (14)	6402 (8)	4561 (11)	76 (7)
C(12)	7334 (11)	5112 (9)	2265 (12)	70 (6)
C(13)	6785 (11)	1503 (9)	−476 (11)	59 (5)
C(14)	5737 (12)	1315 (8)	−891 (11)	60 (5)
C(15)	5938 (17)	1509 (11)	−2270 (13)	92 (8)
C(16)	6234 (15)	2614 (10)	−2461 (12)	92 (8)
C(17)	6394 (11)	3402 (8)	−1252 (10)	55 (5)
C(18)	7522 (11)	3619 (8)	−900 (12)	63 (5)
C(19)	8648 (12)	3048 (13)	−1690 (16)	109 (9)
C(20)	8272 (13)	1912 (12)	−1347 (14)	97 (8)
C(21)	724 (11)	1359 (8)	2023 (13)	62 (6)
C(22)	1831 (11)	1174 (7)	761 (12)	56 (5)
C(23)	1974 (15)	1269 (9)	−649 (13)	83 (8)
C(24)	2175 (14)	2382 (10)	−822 (12)	80 (8)
C(25)	2497 (10)	3218 (8)	242 (11)	54 (5)
C(26)	1450 (12)	3472 (8)	1528 (12)	61 (6)
C(27)	−96 (12)	2886 (11)	1981 (15)	88 (8)
C(28)	−434 (12)	1743 (10)	2119 (18)	97 (9)

[a] Estimated standard deviations are given in parentheses. Coordinates × 10^n where n = 5, 4, and 4 for Ir, N, and C. Temperature parameters × 10^n where n = 4, 3, and 3 for Ir, N, and C. U_{eq} = the equivalent isotropic temperature parameter.

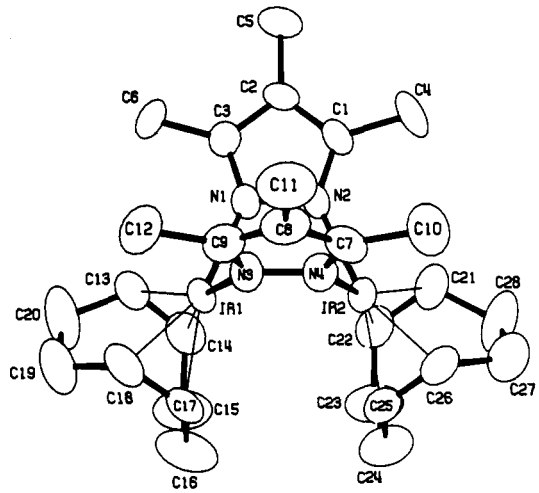

Figure 3. Molecular geometry of compound 9.

Description of the Structures. For each of the molecules 6 and 9, the structure is built around a central nonplanar cyclic core which closely resembles that encountered in analogues we have described previously.[1,2,12] This is illustrated in Figures 2 and 3 (compounds 6 and 9, respectively), two views which are perpendicular to one another across the Ir_2 axis showing the bridging assembly in plan and in profile. The latter (i.e., Figure 3) emphasizes the way in which close approach of the two Ir centers is made possible by bending of the bridging framework into a characteristic[1,2,12] boat-shaped conformation. The other view (Figure 2) also maps the relationship of the various constituent cyclic fragments and shows the way in which the bridge

Table VIII. Selected Structural Data for Compounds 6 and 9

(a) Important Bond Distances and Angles for 6

(i) Bond Distances (Å)

Ir(1)-Ir(2)	3.079 (2)	Ir(2)-N(2)	2.079 (7)
Ir(1)-N(1)	2.100 (7)	Ir(2)-N(4)	2.106 (7)
Ir(1)-N(3)	2.080 (7)	Ir(2)-C(31)	2.119 (9)
Ir(1)-C(21)	2.157 (9)	Ir(2)-C(32)	2.131 (8)
Ir(1)-C(22)	2.140 (9)	Ir(2)-C(35)	2.126 (9)
Ir(1)-C(25)	2.139 (9)	Ir(2)-C(36)	2.140 (11)
Ir(1)-C(26)	2.122 (1)	C=C(av)	1.41[a]
C-C(av)	1.50[a]		

(ii) Bond Angles (deg)

Ir(1)-N(1)-N(2)	112.7 (5)	Ir(2)-N(2)-N(1)	115.6 (5)
Ir(1)-N(1)-C(2)	138.9 (7)	Ir(2)-N(2)-C(4)	137.1 (6)
Ir(1)-N(3)-N(4)	115.3 (5)	Ir(2)-N(4)-N(3)	112.9 (5)
Ir(1)-N(3)-C(14)	136.8 (6)	Ir(2)-N(4)-C(12)	137.3 (7)

(b) Important Bond Distances and Angles for 9

(i) Bond Distances (Å)

Ir(1)-Ir(2)	3.096 (1)	Ir(2)-N(2)	2.072 (7)
Ir(1)-N(1)	2.083 (7)	Ir(2)-N(4)	2.061 (7)
Ir(1)-N(3)	2.057 (7)	Ir(2)-C(21)	2.121 (10)
Ir(1)-C(13)	2.109 (10)	Ir(2)-C(22)	2.110 (9)
Ir(1)-C(14)	2.111 (10)	Ir(2)-C(25)	2.154 (10)
Ir(1)-C(17)	2.139 (10)	Ir(2)-C(26)	2.124 (10)
Ir(1)-C(18)	2.137 (10)	C=C(av)	1.39[a]
C-C(av)	1.50[a]		

(ii) Bond Angles (deg)

Ir(1)-N(1)-N(2)	113.8 (5)	Ir(2)-N(2)-N(1)	114.7 (5)
Ir(1)-N(1)-C(3)	137.7 (5)	Ir(2)-N(2)-C(1)	135.9 (6)
Ir(1)-N(3)-N(4)	115.1 (5)	Ir(2)-N(4)-N(3)	113.9 (5)
Ir(1)-N(3)-C(9)	136.9 (6)	Ir(2)-N(4)-C(7)	135.8 (6)

[a] Within cycloocta-1,5-diene ligand.

3,5 substituents oppose each other along the intermetallic axis, i.e., adopt a relative disposition corresponding to configuration D.

The molecular geometry determined for complex **6**, using material shown by NMR measurements on a recrystallized sample to correspond to that of the major constituent in the diastereoisomeric mixture present in solution, conforms to C_2 point group symmetry and is dissymmetric This situation makes sense on steric grounds, since it might be supposed that the isomer with configuration C (C_s symmetry) might be subject to unfavorable interactions between adjacent 3-phenyl substituents. (In this context it should be noted that the symmetry properties of configuration D vs. C do not allow them to be distinguished from one another on the basis of the spectroscopic data.) Thus the structure of compound **6** offers another[1] way whereby the pyrazolyl-bridged binuclear skeleton may be rendered chiral and offers another[2] example of severe crowding in the vicinity of the axial coordination sites at Ir. The Ir_2 separation at 3.079 (2) Å (Table VIII) is similar to those observed in related dimers incorporating 3,5-disubstituted bridging ligands,[2] more than 0.1 Å shorter than that (3.216 Å) in the parent complex **1**.

An X-ray structure determination for the trimethylpyrazolyl-bridged analogue **9**, which was undertaken because this molecule was among those[5] chosen as subjects for detailed spectroscopic study, proved to be especially useful in that the accuracy achieved allowed structurally significant nonbonding interactions between opposing COD ligands to be clearly identified. Thus while the Ir_2 distance of 3.096 (1) Å is actually longer than those in compound **6** or the μ-fpz species[2] **8**, the COD ethylenic hydrogen atoms attached to C(14), C(22) and C(17), C(25) pairs were located at nonbonding distances of 2.526 and 2.132 Å, respectively, i.e., very short in relation[29] to the van der Waals radius for H. We have suggested that close approach of the corresponding carbon atoms in the structure of compound **8** constitutes indirect evidence for the same kind of interaction.[2] Steric imposition of a lower limit on intermetallic separation by requirements of the terminal diolefin ligands explains why the pronounced contraction along the Ir_2 axis accompanying[1] two-center oxidative addition to compound **20** is not parallelled on oxidation of complex **1** to d^7–d^7 dimers.[12]

Acknowledgment. We thank the N.S.E.R.C., Canada and Imperial Oil Ltd. for financial support, Johnson-Matthey Inc. for a generous loan of iridium trichloride, and NATO for providing a travel grant (to S.A.R.K. and S. R.S.).

Registry No. PzH, 288-13-1; 4-MepzH, 7554-65-6; 3-MepzH, 1453-58-3; 3,5-Me_2pzH, 67-51-6; 3,5-Ph_2pzH, 1145-01-3; 3-Ph-5MepzH, 3347-62-4; fmpzH, 10010-93-2; fpzH, 14704-41-7; 3,4,5-Me_3pzH, 5519-42-6; 3,5-Me_2-4-BrpzH, 3398-16-1; indH, 271-44-3; fbpzH, 95274-69-4; fppzH, 4027-54-7; 4-ClpzH, 15878-00-9; 4-IpzH, 3469-69-0; 4-NO_2pzH, 2075-46-9; **1**, 80462-13-1; **2**, 95274-70-7; **3** (isomer I), 95274-71-8; **3** (isomer II), 95274-72-9; **4**, 95274-73-0; **5**, 95274-74-1; **6** (isomer I), 95274-75-2; **6** (isomer II), 95274-76-3; **7** (isomer I), 86550-48-3; **7** (isomer II), 95274-77-4; **8**, 86550-47-2; **9**, 95274-78-5; **10**, 95274-79-6; **11** (isomer I), 95274-80-9; **11** (isomer II), 95274-81-0; **12**, 95312-99-5; **13**, 95274-87-6; **14**, 95274-82-1; **15**, 95274-83-2; **16**, 95274-84-3; **17**, 87654-05-5; **18**, 82385-06-6; **19**, 77244-03-2; $[Ir(COD)(\mu\text{-}Cl)]_2$, 12112-67-3; $[Rh(COD)(\mu\text{-}Cl)]_2$, 12092-47-6; $[Rh(COD)pzH)_2]PF_6$, 95274-86-5.

Supplementary Material Available: Tables of anisotropic temperature factors, hydrogen atom coordinates and isotropic thermal parameters, bond lengths and angles, and structure factor amplitudes for **6** and **9** (50 pages). Ordering information is given on any current masthead page.

(29) See: Cotton, F. A.; Wilkinson, G. "Advanced Inorganic Chemistry"; 3rd ed.; Interscience: New York, 1972; p 120.